ISSN 2070-0482, Mathematical Models and Computer Simulations, 2019, Vol. 11, No. 5, pp. 690–703. © Pleiades Publishing, Ltd., 2019.
Russian Text © The Author(s), 2019, published in Matematicheskoe Modelirovanie, 2019, Vol. 31, No. 1, pp. 63–84.

Numerical Simulation of Hydrate Formation on Injection of Cold Gas in a Snow Massif

V. Sh. Shagapov[a], A. S. Chiglintseva[a, b, *], and O. A. Shepelkevich[c]

[a] *Mavlyutov Institute of Mechanics, Ufa Federal Research Centre, Russian Academy of Sciences, Ufa, Russia*
[b] *Ufa State Petroleum Technological University, Ufa, Russia*
[c] *Bashkir State University, Ufa, Russia*
**e-mail: changelina@rambler.ru*

Received April 5, 2018; revised April 5, 2018; accepted May 14, 2018

Abstract—The problem on hydrate formation in a snow massif initially saturated with gas with the injection of the same gas is solved. The constructed mathematical model is based on the equations of continuum mechanics. For the axisymmetric formulation with an elongated region of the phase transitions, self-similar solutions are constructed that describe the temperature and pressure fields, as well as the saturation of snow, hydrate, and gas in the massif. The numerical solution of the problem is implemented with the shooting method. It is shown that, depending on the initial thermobaric state of the gas–ice system and on the intensity of gas injection determined by its mass flow rate, three characteristic zones can be distinguished in the filtration area that are different by their structure and elongation: (i) the near zone, in which the snow has completely passed into the hydrate, and, therefore, only the hydrate and gas phases are present; (ii) the intermediate zone, in which the hydrate is formed from gas and ice, and (iii) the distant zone, which is saturated with the gas and ice phases. The effect the mass flow rate of the injected gas, the initial snow saturation, and the initial temperature of the massif have on the elongation of the hydrate volume formation zone under negative temperature conditions and on the temperature and hydration saturation at the boundary separating the near and intermediate zones is studied.

Keywords: gas filtration, snow massif, hydrate formation, axisymmetric formulation, self-similar solution

DOI: 10.1134/S207004821905017X

1. INTRODUCTION

Gas hydrates are solid crystalline compounds (clathrates) generated by water molecules with the main components of natural gas [1]. The hydrates are considered by industrial countries as the most prospective nontraditional source of natural gas, which is associated with significant hydrocarbon reserves in the hydrate form. Hence, in many laboratories, scientific centers, and energy companies throughout the world, studies are currently being carried out related to the possibility of developing such resources.

The advantageous thermobaric conditions for the generation of gas hydrates occur on land in the area of the propagation of perpetually frozen rocks and at the ocean bottom [1–3]. A large-scale research expedition was launched at Lake Baikal in 2009. During the deep submergence of the Mir-2 vehicle, at a depth of 1400 m, extensive hills of gas hydrates were revealed. In total, 44 fields of gas hydrates were discovered at Lake Baikal [2, 3].

More than 230 gas hydrate deposits have been discovered [4, 5]. In 1967 the Messoyakh gas field was discovered in which a gas hydrate deposit was revealed in 1969. Here, the gas reserves are estimated to be up to 30 billion cubic meters [4]. The world's first gas extraction from a hydrate field, located at a depth of 300 m below the sea bottom, was carried out at the beginning of 2013 near Honshu island in Japan [6].

It is well known that gas hydrates may be used as a convenient form for storing and utilizing greenhouse, radioactive, industrial, and other gases, thus avoiding the discharge of harmful substances in the atmosphere [7, 8]. Thus, in 2003 in Japan, Mitsui Engineering & Shipbuilding (MES) first developed a demo project on transportation and storage of natural gas in the form of hydrate granules. In 2009 MES, together with Chugoku Electric Power, constructed the world's first industrial stand for natural gas hydrate production with a 5 ton-per-day capacity [8]. The concept of gas hydrate production using the naturally low temperature conditions of the northern regions of Russia was developed [9]. The experimental results on the fabrication of methane and ethane with a high content of gas in the solid phase under the

free convection conditions in the camera-reactors of the closed type in the water–natural gas and preformed ice–natural gas systems are described in [9].

Nowadays, there are many theoretical and experimental works studying the formation and decomposition of gas hydrates in porous media. In [10] the induction period of hydrate formation at the contact of water and gas was investigated. The temperature fields caused by heat production at hydrate formation at the contact surface between the hydrate massif and gas solution were analyzed. The problem on the extraction of free and hydrate-bonded gas in the desorption mode was solved [11]. The method of gas extraction from the hydrate massif by changing the thermobaric conditions was described. In [12] the principal technological scheme was proposed and a theoretical model was constructed for possible gas extraction from the hydrate massif by pumping warm water. The effect of different regimes of the heat-transfer agent's action on the intensity of gas extraction was studied. In [13] gas hydrate generation in the natural horizon saturated by gas and water as a result of gas injection was numerically studied. The self-similar solutions to the flat one-dimensional problem were constructed that describe the distributions of the main parameters in the horizon. It was established that, depending on the parameters of injected gas, the gas hydrate generation may proceed both on the front surface and in the elongated region. The flat one-dimensional theoretical model for gas hydrate formation on gas injection in a porous reservoir partly saturated with water and in a snow massif saturated by the same gas was considered in [14–16]. The numerical solutions for both the diffusion mechanism and for the equilibrium scheme of hydrate formation were obtained. In [17] the features of gas hydrate formation on gas injection in a porous medium initially filled with gas and ice were studied. The self-similar solutions to the one-dimensional problem that describe the distributions of the main parameters in the reservoir were constructed. It was shown that there are solutions according to which the gas hydrate formation may proceed in three different regimes. In [18] hydrate generation from ice on gas injection in a porous medium was studied. The numerical solution to the problem was obtained with the method of front tracking in the mesh node. The effects of ice saturation and the parameters at the medium's boundary on the peculiarities of the process were analyzed. In [19] the gas hydrate formation on gas injection into a porous medium partly saturated with water was studied in the flat one-dimensional self-similar formulation. The effects of a porous medium's initial parameters (porosity, permeability, and water content), temperature, and intensity of gas injection on the pattern of hydrodynamic and temperature fields in the porous medium were analyzed. It was shown that, depending on the intensity of cold gas injection into a wet porous medium, the process may proceed in several regimes with a qualitatively different structure of hydrate formation zones. In [20] the problem on the injection of a warm hydrate-forming gas in a snow massif initially saturated by the same gas was solved at the transition of the gas–snow system through the melting point of ice.

The goal of this work is to study the injection of a cold hydrate-forming gas in a snow massif saturated by the same gas in the axisymmetric formulation before the melting temperature of ice is reached in the system. This work is an extension of the studies performed in the papers [17, 20–23], where the mathematical models were constructed in a rectilinear-parallel approximation. In the current work, we took into account the effect of conductive and convective components in the heat transfer equation in simulating the process of hydrate formation in the intermediate zone. Here, to describe the fields of pressure and hydrate saturation, we used the system of nonlinearized differential equations, while in [24] the approximate analytical solution for the distribution of these fields in the spatial domain was obtained with the Laybenson linearization. The results obtained by solving this kind of problem are some initial stage of gas hydrate formation in massifs and horizons of finite length and may be used to test the chosen numerical algorithms.

2. PROBLEM FORMULATION AND MAIN EQUATIONS

We assume that we have a homogeneous horizontal snow massif of constant thickness and unbounded elongation initially saturated by gas S_{g0} at pressure p_0 and temperature T_0 corresponding to the thermodynamic conditions of the existence of these phases in the free state. We also assume that, for the initial state of the gas–ice system, the initial temperature T_0 is below the melting point of ice ($T_0 < T^{(0)}, T^{(0)} = 0$°C) and pressure p_0 is less than the equilibrium pressure of phase transitions $p_s(T_0)$ of the gas–ice–hydrate system [20, 21]:

$$T = T_0, \quad p = p_0, \quad p_0 < p_s(T_0), \quad S_i = S_{i0}, \quad S_g = S_{g0}, \quad S_h = 0 \quad (t = 0,\ 0 < r < \infty). \tag{1}$$

We assume the top and the bottom of the massif are impermeable and are weak conductors of heat. Let a well be drilled in the massif of radius $r = r_w$ and let this well penetrate the massif through its entire thickness. We assume cold gas (the same as the initial one) is pumped through the well with a constant mass flow rate Q_g related to the well length unit (the current pressure at the well boundary is $p_{(w)}$) and constant temperature T_g ($T_{(w)} = T_g \le 0$°C).

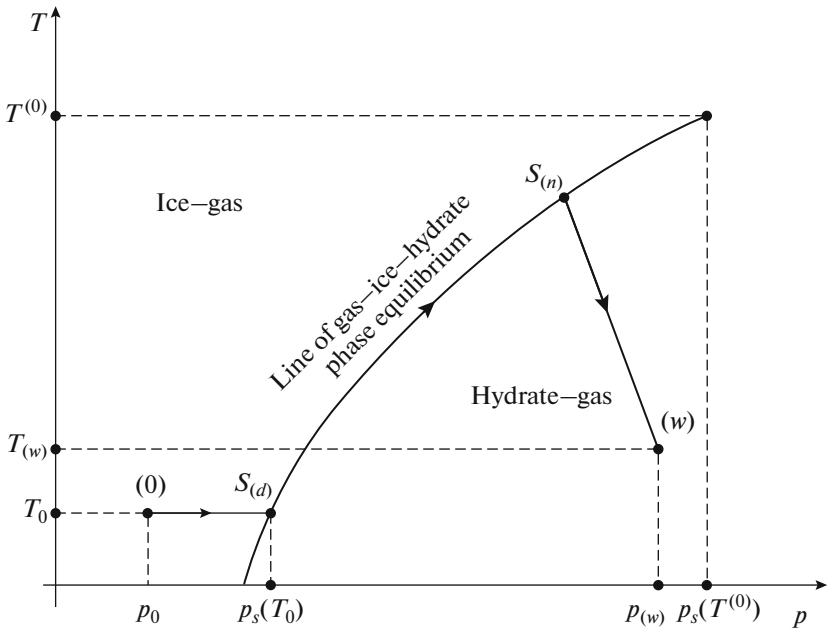

Fig. 1. Scheme of gas injection in snow massif in which ice melting temperature ($T^{(0)} = 0°C$) is not reached. Scheme is drawn in pressure–temperature plane (p, T).

Depending on the initial thermobaric state of the gas–ice system and on the intensity of the gas injection determined by the mass flow rate Q_g, we will assume that in the gas filtration zone ($r > r_{(w)}$),three characteristic zones may appear: the near zone, where only the gas and hydrate occur, the intermediate zone, where gas and snow transit into the hydrate compound and are in the phase equilibrium state, and the distant zone, filled with gas and snow. Consequently, two front boundaries are introduced here: between the distant and intermediate zones, where the transition of gas and ice into the hydrate compound begins, and between the near and intermediate zones, where the hydrate formation process terminates.

Figure 1 illustrates the gas injection in the massif saturated by snow and gas in the phase plane pressure–temperature (p, T). The boundary condition at $r = r_{(w)}$ is marked by point (w). The points $s_{(n)}$ and $s_{(d)}$ on the curve of the phase equilibrium of the gas–ice–hydrate system correspond to the near and distant boundaries of the intermediate zone. The line segment between these points on the line of the phase equilibrium corresponds to the intermediate zone, whereas the segments between (w) and $s_{(n)}$ and between $s_{(d)}$ and (0) correspond to the near and distant zones, respectively. The initial state of the massif saturated by gas and snow is marked in the phase diagram by point (0). Here, when a certain value of pressure in the massif $p_s(T_0)$ is reached, due to the gas injection corresponding to the condition of hydrate formation for the current temperature T_0, the snow and gas transition into the hydrate state; the intermediate zone is formed, and the front boundary (denoted in the phase plane by the point $s_{(d)}$), at which the process of hydrate formation begins, appears. Since the gas is injected at the temperature and pressure outside the zone of hydrate stability ($p_{(w)} > p_s(T_{(w)})$), the near zone saturated only by the gas and hydrate will be generated. Consequently, the second moving boundary between the near and intermediate zones, at which the hydrate formation process terminates, appears (it is denoted by the point $s_{(n)}$).

We will assume snow and hydrate are incompressible and we assume the gas is calorically perfect:

$$\rho_i, \rho_h = \text{const}, \quad p = \rho_g R_g T. \tag{2}$$

Here, the filtration and heat transfer are accompanied by the gas and ice transitions to the hydrate state. In this case the system of governing equations is the system of laws of gas and snow mass conservation,

heat transfer, and gas filtration. This system in the axisymmetric approximation takes the form [17, 20, 24–30]:

$$\frac{\partial}{\partial t}(S_g\rho_g) + \frac{1}{r}\frac{\partial}{\partial r}(rS_g\rho_g\upsilon_g) = -\rho_h G\frac{\partial S_h}{\partial t},$$

$$\frac{\partial}{\partial t}(S_i\rho_i) = -\rho_h(1-G)\frac{\partial S_h}{\partial t},$$

$$\frac{\partial}{\partial t}(\rho c T) + \rho_g c_g S_g \upsilon_g \frac{\partial T}{\partial r} = \frac{1}{r}\frac{\partial}{\partial r}\left(r\lambda\frac{\partial T}{\partial r}\right) + \rho_h l_h \frac{\partial S_h}{\partial t}, \tag{3}$$

$$S_g\upsilon_g = -\frac{k_g}{\mu_g}\frac{\partial p}{\partial r},$$

$$(\rho c = \rho_g S_g c_g + \rho_h S_h c_h + \rho_i S_i c_i,\ \lambda = \lambda_g S_g + \lambda_h S_h + \lambda_i S_i),$$

where G is the mass concentration of the gas in the hydrate; ρ_j and S_j ($j = h, i, g$) are the true densities and saturations of the jth phase; indices h, i, and g are related to the hydrate, snow, and gas; υ_g, k_g, c_g, and μ_g are the velocity, permeability, specific heat conductivity at constant volume, and dynamical viscosity of the gas phase; p is the pressure; T is the temperature; l_h is the specific heat of hydrate formation related to its mass unit; and ρc and λ are the specific heat per unit volume and heat transfer coefficient of the gas–ice–hydrate system.

The phase saturations must satisfy the condition [26]:

$$S_g + S_i + S_h = 1. \tag{4}$$

Because in the work we consider sufficiently long time scales which significantly exceed the characteristic time of the diffusion kinetics of the process, we take the equilibrium scheme of hydrate formation, which suggests that its intensity is limited by the removal of the latent heat of hydrate formation. Therefore, in the zone where ice, gas, and hydrate occur simultaneously, the condition of phase equilibrium must be satisfied; i.e., the temperature and current pressure value are linked by the following relation [20–22]:

$$T_s(p) = T_{(s0)} + T_* \ln(p/p_{(s0)}), \tag{5}$$

where $T_{(s0)}, T_*$, and $p_{(s0)}$ are the empirical parameters depending both on the type of gas hydrate and on the considered ranges of temperature and pressure ($T_{(s0)}$ is the equilibrium temperature at $p = p_{(s0)}$) [16].

At the boundaries between the considered zones, where the phase saturations and mass and heat flows spike, the relations are fulfilled which follow from the conditions of the mass and heat balance [24, 25]:

$$\begin{gathered}\left[(S_h\rho_h(1-G) + S_i\rho_i)\dot r_{(s)}\right] = 0,\\ \left[\rho_g S_g(\upsilon_g - \dot r_{(s)}) - \rho_h S_h G\dot r_{(s)}\right] = 0,\\ \left[\lambda\frac{\partial T}{\partial r}\right] = \left[\rho_h l_h S_h \dot r_{(s)}\right].\end{gathered} \tag{6}$$

Here, $[\psi]$ is the jump in parameter ψ at the boundary between the zones $r = r_{(s)}$ ($s = n, d$), $\dot r_{(s)}$ is the velocity of this boundary, $s = n$ is related to the boundary between the near and intermediate zones, and $s = d$ is related to the boundary between the intermediate and distant zones.

As a result of gas injection, a zone saturated by gas and hydrate is generated near the well. Considering sufficiently long time periods after the start of the gas injection, when the dimensions of this zone significantly exceed the well radius ($r_{(s)} \gg r_w$), we can show that its dimension sufficiently weakly affects the peculiarities of the considered process. Then, taking the Darcy law into account (the fourth equation in (3)) and for the equation of state for gas (2), we write the conditions at the well boundary ($r = r_w$) in the form

$$-\frac{k_g\pi}{\mu_g R_g T_g}\left(r\frac{\partial p^2}{\partial r}\right) = Q_g = \text{const},\quad T_{(w)} = T_e = \text{const}\ (r_w \to 0,\ t > 0). \tag{7}$$

3. SOLUTIONS IN THE NEAR AND DISTANT ZONES

From the first equation in system (3), taking into account the Darcy law (the fourth equation in system (3)) and Eq. (2), as well as the fact that the gas and hydrate saturations are constant ($S_g, S_h = \text{const}$), we obtain the piezoconductivity equation for the near zone ($r_w < r < r_{(n)}$)

$$\frac{\partial p}{\partial t} = \frac{1}{r}\frac{\partial}{\partial r}\left(r \frac{k_g}{\mu_g S_{ge}} p \frac{\partial p}{\partial r}\right). \tag{8}$$

We integrate the second equation in system (3) with the initial condition (1) and obtain

$$S_h = \frac{\rho_i}{\rho_h(1-G)}(S_{i0} - S_i), \quad S_g = 1 - S_{i0} + \left(1 - \frac{\rho_i}{\rho_h(1-G)}\right)(S_{i0} - S_i). \tag{9}$$

Since in the near zone all the snow transits into the hydrate compound ($S_i = 0$), from (9) we obtain the expression for the saturation of the hydrate:

$$S_{he} = \frac{\rho_i S_{i0}}{\rho_h(1-G)}, \quad S_{ge} = 1 - S_{he}. \tag{10}$$

From the third equation in system (3), taking the Darcy law into account, we obtain the equation of heat conductivity for the near zone ($r_w < r < r_{(n)}$):

$$\frac{\partial}{\partial t}(\rho c T) = \rho_g c_g \frac{k_g}{\mu_g}\frac{\partial p}{\partial r}\frac{\partial T}{\partial r} + \frac{1}{r}\frac{\partial}{\partial r}\left(r \lambda_{(1)} \frac{\partial T}{\partial r}\right). \tag{11}$$

In the distant zone ($r_{(d)} < r < \infty$), the calorically perfect gas without hydrate formation is filtrated; therefore, the change in temperature is insignificant. Then, from the continuity equation for gas (the first equation in system (3)), taking into account the Darcy law, and assuming $T = T_0, S_h = 0$, and the equation of state (2), we derive the nonlinear filtration equation in the following form:

$$\frac{\partial p}{\partial t} = \frac{1}{r}\frac{\partial}{\partial r}\left(r \frac{k_g}{\mu_g S_{g0}} p \frac{\partial p}{\partial r}\right). \tag{12}$$

4. EQUATION OF PIEZOCONDUCTIVITY IN THE INTERMEDIATE ZONE

The second equation in system (3) taking (4) into account may be reduced to the form

$$\frac{\partial S_g}{\partial t} = \left(\frac{\rho_h(1-G)}{\rho_i} - 1\right)\frac{\partial S_h}{\partial t}. \tag{13}$$

We substitute (13) into the first equation in system (3), use the Darcy law and equation of state for gas (2), and obtain the following equation for the variation in hydrate saturation in the intermediate zone:

$$\frac{\partial S_h}{\partial t} = \left(\frac{1}{r}\frac{\partial}{\partial r}\left(\frac{k_g}{\mu_g}\frac{p}{R_g T_s(p)}\frac{\partial p}{\partial r}\right) - S_g \frac{\partial}{\partial t}\left(\frac{p}{R_g T_s(p)}\right)\right)\Big/\tilde{\rho}, \tag{14}$$

where $\tilde{\rho} = \dfrac{p}{R_g T_s(p)}\left(\dfrac{\rho_h(1-G)}{\rho_i} - 1\right) + \rho_h G$.

From the equation of heat transfer (the third equation in system (3)), taking into account the Darcy law (the fourth equation in system (3)), expression (14), and the condition of phase equilibrium (5), we obtain

$$\begin{aligned} \rho c \frac{T_*}{p}\frac{\partial p}{\partial t} - \frac{c_g k_g T_*}{R_g T_s(p)\mu_g}\left(\frac{\partial p}{\partial r}\right)^2 &= \frac{\lambda T_*}{rp}\left(\frac{\partial p}{\partial r} + r\left(\frac{\partial^2 p}{\partial r^2} - \frac{1}{p}\left(\frac{\partial p}{\partial r}\right)^2\right)\right) \\ + \frac{\rho_h l_h}{\tilde{\rho} R_g T_s(p)}\left[\frac{k_g}{\mu_g r}\left(\frac{r\left(T_s(p) - T_*\right)}{T_s(p)}\left(\frac{\partial p}{\partial r}\right)^2 + p\frac{\partial p}{\partial r} + rp\frac{\partial^2 p}{\partial r^2}\right) - S_g \frac{\left(T_s(p) - T_*\right)}{T_s(p)}\frac{\partial p}{\partial t}\right]. \end{aligned} \tag{15}$$

The corresponding temperature distribution is related to the pressure in the intermediate zone by the phase equilibrium condition, Eq. (5).

We integrate (13) with the initial conditions (1) and obtain the expression where the current value of gas saturation depends on the current value of hydrate saturation in the intermediate zone:

$$S_g = S_{g0} - \left(1 - \frac{\rho_h(1-G)}{\rho_i}\right) S_h.$$

5. BOUNDARY CONDITIONS BETWEEN ZONES

From the conservation conditions on the boundaries between the zones, Eq. (6), after taking the Darcy law for the near boundary ($r = r_{(n)}$) into account, we obtain [24, 25]

$$-\frac{k_g}{\mu_g}\left(\frac{\partial p}{\partial r}\right)^{-}_{(n)} + \frac{k_g}{\mu_g}\left(\frac{\partial p}{\partial r}\right)^{+}_{(n)} = \left(\left(S^{-}_{g(n)} - S^{+}_{g(n)}\right) + \frac{\rho_h G}{\rho_{g(n)}}\left(S^{-}_{h(n)} - S^{+}_{h(n)}\right)\right)\dot{r}_{(n)}. \tag{16}$$

From now on the upper indices (–) and (+) indicate the parameter values at the jump before and behind the boundary.

The heat balance condition (the third expression in (6)) is now written in the form

$$\left(\lambda_{(1)}\frac{\partial T}{\partial r}\right)^{-}_{(n)} - \left(\lambda_{(2)}\frac{\partial T}{\partial r}\right)^{+}_{(n)} = \rho_h l_h \left(S^{-}_{h(n)} - S^{+}_{h(n)}\right)\dot{r}_{(n)}. \tag{17}$$

The phase saturations are coupled by the following relations:

$$S^{-}_{h(n)} = S_{h(\mathrm{e})},\ S^{-}_{g(n)} = S_{g(\mathrm{e})},\ S^{+}_{g(n)} = 1 - S_{i0} - \left(1 - \rho_h(1-G)/\rho_i\right) S^{+}_{h(n)}. \tag{18}$$

At the distant boundary ($r = r_{(d)}$) we assume that the hydrate saturation has no jump ($S^{-}_{h(d)} = S^{+}_{h(d)} = 0$); then, from conditions (6) at $r = r_{(d)}$, we deduce

$$-\left(\frac{\partial p}{\partial r}\right)^{-}_{(d)} + \left(\frac{\partial p}{\partial r}\right)^{+}_{(d)} = 0. \tag{19}$$

In the intermediate zone ($r_{(n)} < r < r_{(d)}$), the temperature and pressure are linked by the condition of phase equilibrium, Eq. (5); therefore, the corresponding derivatives at the front boundaries $r = r_{(n)}$ and $r = r_{(d)}$ must be linked by the following relations:

$$\left(\frac{\partial T}{\partial r}\right)^{+}_{(n)} = \frac{T_*}{p_{(n)}}\left(\frac{\partial p}{\partial r}\right)^{+}_{(n)} \quad \text{and} \quad \left(\frac{\partial T}{\partial r}\right)^{-}_{(d)} = \frac{T_*}{p_{(d)}}\left(\frac{\partial p}{\partial r}\right)^{-}_{(d)}. \tag{20}$$

6. SELF-SIMILAR SOLUTIONS

We introduce the self-similar variable [20, 31]

$$\xi = r\Big/\left(2\sqrt{\chi_0^{(p)} t}\right), \tag{21}$$

where $\chi_0^{(p)} = k_g p_0/(S_{g0}\mu_g)$ is the coefficient of piezoconductivity.

By ignoring the temperature variation in the near zone (because in this zone the condition $\Delta T/T \ll 1$ is satisfied for the temperature in the Kelvin scale) and by applying the Laybenson linearization [17, 20] in the continuity equations (8) and (12), in the self-similar variables from (8), (11), and (12) we can transform the system into

$$\begin{gathered}
-\left(\xi + \frac{S_{g0}}{2S_{ge}}\frac{1}{\xi}\right)\frac{dp^2_{(1)}}{d\xi} = \frac{S_{g0}}{2S_{ge}}\frac{d^2 p^2_{(1)}}{d\xi^2}, \\
-\xi\frac{dT_{(1)}}{d\xi} = \frac{\mathrm{Pe}_{(1)}\varphi_{(1)}}{p_0{}^2}\frac{dp^2_{(1)}}{d\xi}\frac{dT_{(1)}}{d\xi} + 2\varphi_{(1)}\left(\frac{1}{\xi}\frac{dT_{(1)}}{d\xi} + \frac{d^2 T_{(1)}}{d\xi^2}\right), \\
-\left(\xi + \frac{1}{2\xi}\right)\frac{dp^2_{(3)}}{d\xi} = \frac{1}{2}\frac{d^2 p^2_{(3)}}{d\xi^2},
\end{gathered} \tag{22}$$

where $\varphi_{(1)} = \chi^{(T)}/4\chi_0^{(p)}$, $\mathrm{Pe}_{(1)} = \rho_{g0}c_g k_g p_0/(\lambda_{(1)}\mu_g)$ is the Péclet number and $\chi^{(T)} = \lambda_{(1)}/(\rho c)$ is the coefficient of temperature conductivity. From now on the lower indices 1, 2, and 3 are related to the near, intermediate, and distant zones, respectively.

We integrate the first and the second equations in (22) for the pressure and temperature distributions in the near zone ($0 < \xi < \xi_{(n)}$) with the boundary conditions (7) and obtain the following solutions:

$$p_{(1)}^2 = p_{(n)}^2 + \frac{Q_g \mu_g R_g T_g}{k_g \pi}\int_{\xi}^{\xi_{(n)}} \frac{1}{\xi}\exp\left(-\frac{\xi^2}{\eta_{(1)}}\right)d\xi, \tag{23}$$

$$T_{(1)} = T_{(n)} + \frac{\left(T_g - T_{(n)}\right)\int\limits_{\xi}^{\xi_{(n)}} \frac{1}{\xi}\exp\left(-\frac{\xi^2}{4\varphi_{(1)}} - \frac{\mathrm{Pe}_{(1)}}{2p_0^2}p_{(1)}^2\right)d\xi}{\int\limits_{0}^{\xi_{(n)}} \frac{1}{\xi}\exp\left(-\frac{\xi^2}{4\varphi_{(1)}} - \frac{\mathrm{Pe}_{(1)}}{2p_0^2}p_{(1)}^2\right)d\xi},$$

where $\eta_{(1)} = S_{g0}/S_{g(\mathrm{e})}$.

For the distant zone ($\xi_{(d)} < \xi < \infty$) with the initial conditions (1), we can write

$$p_{(3)}^2 = p_0^2 + \frac{\left(p_{(d)}^2 - p_0^2\right)\int\limits_{\xi}^{\infty} \frac{1}{\xi}\exp(-\xi^2)d\xi}{\int\limits_{\xi_{(d)}}^{\infty} \frac{1}{\xi}\exp(-\xi^2)d\xi}. \tag{24}$$

For the intermediate zone, we rewrite Eqs. (14) and (15) in the self-similar coordinate in the form

$$\frac{d^2 p_{(2)}}{d\xi^2} = \frac{B\frac{dp_{(2)}}{d\xi} + C\left(\frac{dp_{(2)}}{d\xi}\right)^2}{A}, \tag{25}$$

$$\frac{dS_{h(2)}}{d\xi} = -\frac{1}{\tilde{\rho}\xi R_g T_s(p_{(2)})}\left[\frac{k_g}{2\mu_g\chi_0^{(p)}}\left(p_{(2)}\frac{d^2p_{(2)}}{d\xi^2} + \left(1 - \frac{T_*}{T_s(p_{(2)})}\right)\left(\frac{dp_{(2)}}{d\xi}\right)^2 + \frac{p_{(2)}}{\xi}\frac{dp_{(2)}}{d\xi}\right) + S_g\xi\left(1 - \frac{T_*}{T_s(p_{(2)})}\right)\left(\frac{dp_{(2)}}{d\xi}\right)\right], \tag{26}$$

$$A = \frac{1}{\chi_0^{(p)}}\left(\lambda + \frac{\rho_h l_h p_{(2)}^2 k_g}{\tilde{\rho}R_g T_s\,(p_{(2)})T_*\mu_g}\right),$$

$$B = -2\rho c\xi - \frac{\lambda}{\xi\chi_0^{(p)}} - \frac{\rho_h l_h p_{(2)}}{\tilde{\rho}R_g T_s(p_{(2)})T_*}\left(\frac{k_g p_{(2)}}{\mu_g\xi\chi_0^{(p)}} + \frac{2S_g\left(T_s(p_{(2)}) - T_*\right)\xi}{T_s(p_{(2)})}\right),$$

$$C = \frac{1}{\chi_0^{(p)}}\left(\frac{\lambda}{p_{(2)}} - \frac{p_{(2)}k_g c_g}{R_g\mu_g T_s\,(p_{(2)})} - \frac{\rho_h l_h p_{(2)}k_g\left(T_s\,(p_{(2)}) - T_*\right)}{\tilde{\rho}R_g T_s^2(p_{(2)})T_*\mu_g}\right).$$

Conditions (16) and (17) for the near boundary ($\xi = \xi_{(n)}$) in the self-similar coordinate become

$$-\left(\frac{dp}{d\xi}\right)_{(n)}^{-} + \left(\frac{dp}{d\xi}\right)_{(n)}^{+} = \frac{2\chi_0^{(p)}\mu_g}{k_g}\left((S_{g(n)}^{-} - S_{g(n)}^{+}) + \frac{\rho_h G}{\rho_{g(n)}}(S_{h(n)}^{-} - S_{h(n)}^{+})\right)\xi_{(n)}, \tag{27}$$

$$\lambda_{(1)}\left(\frac{dT}{d\xi}\right)_{(n)}^{-} - \lambda_{(2)}\left(\frac{dT}{d\xi}\right)_{(n)}^{+} = 2\rho_h l_h\chi_0^{(p)}(S_{h(n)}^{-} - S_{h(n)}^{+})\xi_{(n)}. \tag{28}$$

The first relationship from (20) in the self-similar coordinates takes the form

$$\left(\frac{dT}{d\xi}\right)^{+}_{(n)} = \frac{T_*}{p_{(n)}}\left(\frac{dp}{d\xi}\right)^{+}_{(n)}. \tag{29}$$

Using the analytical solutions (23) and relation (29), we may transform conditions (27) and (28) to the form

$$\frac{Q_g \mu_g R_g T_g}{2p_{(n)} k_g \pi \xi_{(n)}} \exp\left(-\frac{\xi^2_{(n)}}{\eta_{(1)}}\right) + q_{(n)} = \frac{2\chi_0^{(p)} \mu_g \xi_{(n)}}{k_g}\left((S^-_{g(n)} - S^+_{g(n)}) + \frac{\rho_h G}{\rho_{g(n)}}(S^-_{h(n)} - S^+_{h(n)})\right), \tag{30}$$

$$\frac{\lambda_{(1)}(T_{(n)} - T_g)\dfrac{1}{\xi_{(n)}}\exp\left(-\dfrac{\xi^2_{(n)}}{4\varphi_{(1)}} - \dfrac{\mathrm{Pe}_{(1)} p^2_{(n)}}{2p_0^2}\right)}{\displaystyle\int_0^{\xi_{(n)}} \frac{1}{\xi}\exp\left(-\frac{\xi^2}{4\varphi_{(1)}} - \frac{\mathrm{Pe}_{(1)} p^2_{(1)}}{2p_0^2}\right) d\xi} - \lambda_{(2)}\frac{T_* q_{(n)}}{p_{(n)}} = 2\rho_h l_h \chi_0^{(p)}\left(S^-_{h(n)} - S^+_{h(n)}\right)\xi_{(n)}, \tag{31}$$

$$q_{(n)} = \left(\frac{dp_{(2)}}{d\xi}\right)_{\xi_{(n)}}.$$

We express $T_{(n)}$ from the condition of phase equilibrium, Eq. (5), through $p_{(n)}$, substitute it into condition (29), and derive at the near boundary $\xi = \xi_{(n)}$ the following relations associating the unknown parameter $q_{(n)}$, value of boundary coordinate $\xi_{(n)}$, and pressure $p_{(n)}$ at this boundary:

$$\psi_1(\xi_{(n)}, p_{(n)}, q_{(n)}) = \frac{Q_g \mu_g R_g T_g}{2p_{(n)} k_g \pi \xi_{(n)}} \exp\left(-\frac{\xi^2_{(n)}}{\eta_{(1)}}\right) + q_{(n)} - \frac{2\chi_0^{(p)} \mu_g}{k_g}\xi_{(n)}\left((S^-_{g(n)} - S^+_{g(n)}) + \frac{\rho_h G}{\rho_{g(n)}}(S^-_{h(n)} - S^+_{h(n)})\right), \tag{32}$$

$$\psi_2(\xi_{(n)}, p_{(n)}, q_{(n)}) = \frac{\lambda_{(1)}\left(T_{(n)} - T_g\right)\dfrac{1}{\xi_{(n)}}\exp\left(-\dfrac{\xi^2_{(n)}}{4\varphi_{(1)}} - \dfrac{\mathrm{Pe}_{(1)} p^2_{(n)}}{2p_0^2}\right)}{\displaystyle\int_0^{\xi_{(n)}} \frac{1}{\xi}\exp\left(-\frac{\xi^2}{4\varphi_{(1)}} - \frac{\mathrm{Pe}_{(1)} p^2_{(1)}}{2p_0^2}\right) d\xi} - \lambda_{(2)}\frac{T_*}{p_{(n)}} q_{(n)} - 2\rho_h l_h \chi_0^{(p)}(S^-_{h(n)} - S^+_{h(n)})\xi_{(n)}. \tag{33}$$

At the boundary $\xi = \xi_{(d)}$, we rewrite condition (19)

$$\left(\frac{dp}{d\xi}\right)^{-}_{(d)} = \left(\frac{dp}{d\xi}\right)^{+}_{(d)}. \tag{34}$$

For the intermediate zone ($\xi_{(n)} \le \xi \le \xi_{(d)}$) the equations, which are the system of three ordinary differential equations (25) and (26), may be transformed into

$$\frac{dp_{(2)}}{d\xi} = q,$$

$$\frac{dq}{d\xi} = \frac{Bq + Cq^2}{A}, \tag{35}$$

$$\frac{dS_{h(2)}}{d\xi} = -\frac{1}{\tilde{\rho}\xi R_g T_s(p_{(2)})}\left[\frac{k_g}{2\mu_g \chi_0^{(p)}}\left(p_{(2)}\frac{dq}{d\xi} + \left(1 - \frac{T_*}{T_s(p_{(2)})}\right)q^2 + \frac{p_{(2)}}{\xi}q\right) + S_g \xi\left(1 - \frac{T_*}{T_s(p_{(2)})}\right)q\right].$$

The calculation of the system of ordinary differential equations, Eq. (35), begins from the right boundary $\xi = \xi_{(d)}$ whose value is chosen arbitrarily towards the left boundary $\xi = \xi_{(n)}$ with a negative step. Here, the unknown parameters are the values of the function $q_{(n)}$, coordinates of the frontal boundaries $\xi_{(n)}$ and

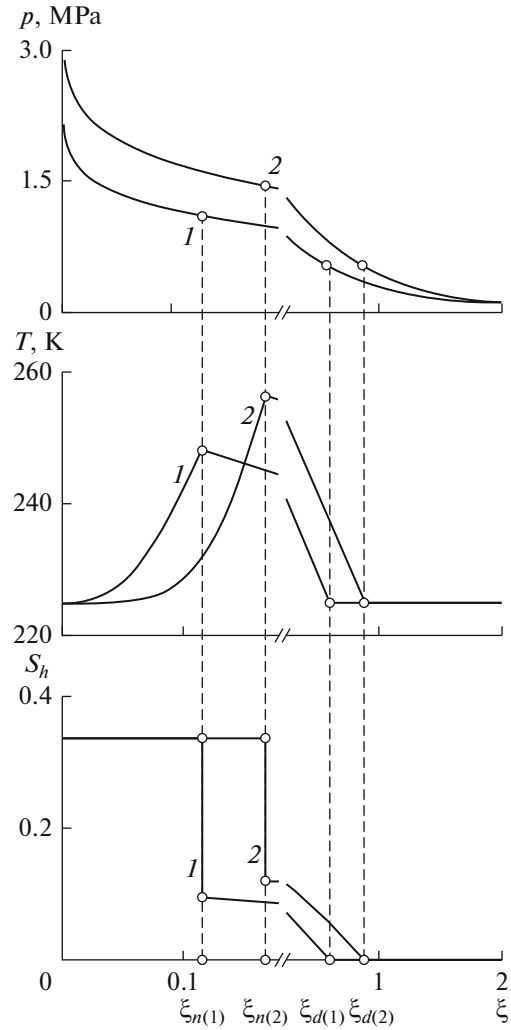

Fig. 2. Distributions of pressure p, temperature T, and hydrate saturation S_h in massif for different gas mass flow rates Q_g: *1* is for 2×10^{-3}, *2* is for 3×10^{-3}, and *3* is for 4×10^{-3} kg/(m s).

$\xi_{(d)}$, and the pressure values at these boundaries $p_{(n)}$ and $p_{(d)}$. As the initial Cauchy data at the distant boundary $\xi = \xi_{(d)}$, we may take the following values:

$$p_{(d)} = p_s(T_0), \quad q_{(d)} = \left(\frac{dp}{d\xi}\right)^{+}_{(d)}, \quad S_h = 0. \tag{36}$$

Following from equality (36) and using solution (24) for the distant zone, the value $q_{(d)}$ is determined based on the expression

$$q_{(d)} = (p_0^2 - p_{(d)}^2)\frac{\exp(-\xi_{(d)}^2)}{2p_{(d)}\xi_{(d)}\int\limits_{\xi_{(d)}}^{\infty}\frac{1}{\xi}\exp(-\xi^2)d\xi}. \tag{37}$$

The numerical solution to the problem was determined by the shooting method [17, 24]. In the computations, instead of values $\xi_{(n)}$, $p_{(n)}$, and $q_{(n)}$ in (32) and (33), we substitute the current values ξ, p, and q obtained by the integration of system (33). Each computation variant is terminated when ψ_1 reaches the zero value ($\psi_1(\xi_{(n)}, p_{(n)}, q_{(n)}) = 0$). Shooting by parameter $\xi_{(d)}$ is continued before achieving the condition $\psi_2(\xi_{(n)}, p_{(n)}, q_{(n)}) = 0$ with some prescribed degree of accuracy.

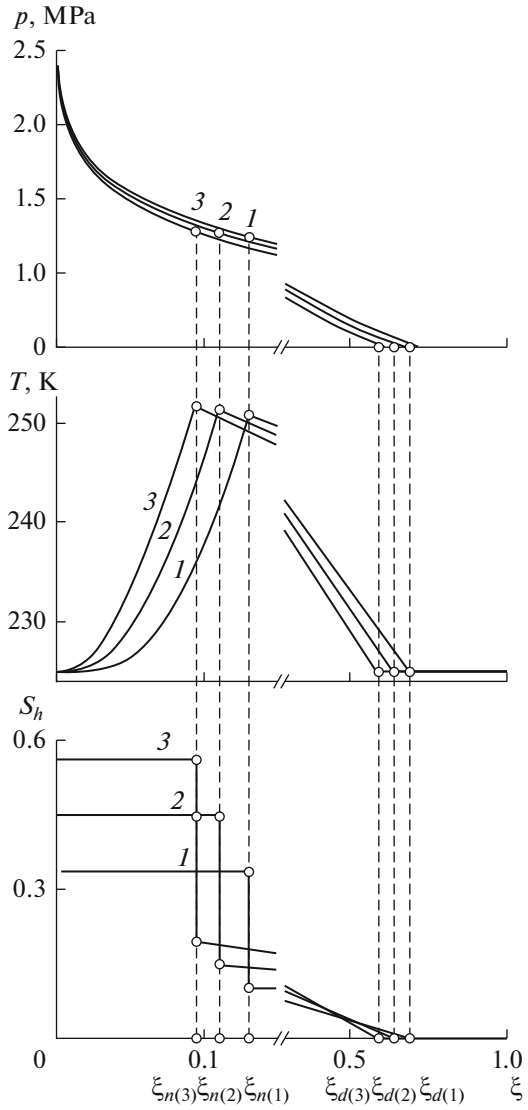

Fig. 3. Distributions of pressure p, temperature T, and hydrate saturation S_h in massif for different initial values of snow saturation S_{i0}: *1* is for 0.3, *2* is for 0.4, and *3* is for 0.5.

7. CALCULATIONS

We took the following values for the parameters determining the properties of the snow, gas, and hydrate phases: $\rho_i = 900$ kg/m^3, $\rho_h = 910$ kg/m^3, $c_g = 1650$ J/(kg K), $c_i = 2090$ J/(kg K), $c_h = 2200$ J/(kg K), $\lambda_g = 0.03$ W/(m K), $\lambda_i = 2$ W/(m K), $\lambda_h = 0.5$ W/(m K), $l_h = 1.45\times10^5$ J/kg, $G = 0.12$, $\mu_g = 9.5\times10^{-6}$ Pa s, $k_g = 10^{-15}$ m^2, $R_g = 520$ J/(kg K), $T_{(s0)} = 263$ K, $p_{(s0)} = 1.86$ MPa, and $T_* = 30$ K.

The initial values of the pressure and temperature of the snow massif and injected gas with the constant mass rate $Q_g = 2\times10^{-3}$ kg/(m s) were chosen equal to $p_0 = 0.1$ MPa, $T_0 = 225$ K, and $T_e = 225$ K. The initial snow saturation is $S_{i0} = 0.3$.

The distributions of pressure p, temperature T, and hydrate saturation S_h in the massif at different mass flow rates of the gas are illustrated in Fig. 2. From the graph it is seen that, as the mass flow rate of the injected gas is increased, which corresponds to the increase in pressure of the injected gas, the elongation of the hydrate formation zone increases, because the intensity of the gas supply increases, which leads to the growth in hydrate saturation at the near boundary. Note that the temperature in the massif also increases, associated with the increase in the pressure which leads—according to expression (5)—to the

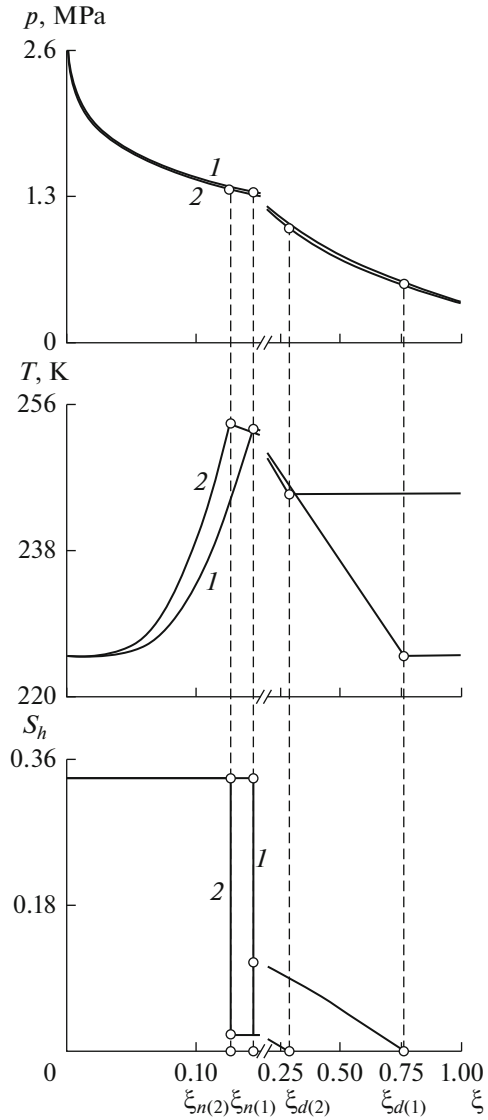

Fig. 4. Distributions of pressure p, temperature T, and hydrate saturation S_h in massif for different initial values of massif temperature T_0: *1* is for 225 and *2* is for 245 K.

growth in the equilibrium temperature of the hydrate formation. The chosen scheme with two moving interphase boundaries allows constructing physically noncontradictory solutions. From the figure we can see that, according to the taken values of the gas mass flow rate, the maximum temperature in the massif does not reach the ice melting temperature ($T^{(0)} = 0$°C), which excludes the appearance of water in the massif. In the case of larger values of the gas flow rate leading to an increase in the pressure at the well boundary and, respectively, to an increase in the temperature in the massif, which may be higher than the ice melting temperature, we should consider an additional zone where the hydrate is formed from the gas and water along the phase equilibrium curve.

Figure 3 presents similar distributions as in Fig. 2 for different initial values of snow saturation in the massif S_{i0}. It is shown that, as the snow saturation grows in the massif, the elongation of the spatial zone of hydrate formation decreases, because, at the given mass flow rate of the gas, the fraction of its consumption needed for hydrate formation increases, which in turn leads to a faster decrease in the pressure; an insignificant increase in temperature in the massif is also noted here.

Figure 4 presents the analogous distributions as in Fig. 2 for different values of the initial temperature T_0 of the massif. The numbers on curves *1* and *2* correspond to the values 225 and 245 K. We can see that in the case of low-temperature massifs, at the given intensity of gas injection, the elongation of the spatial

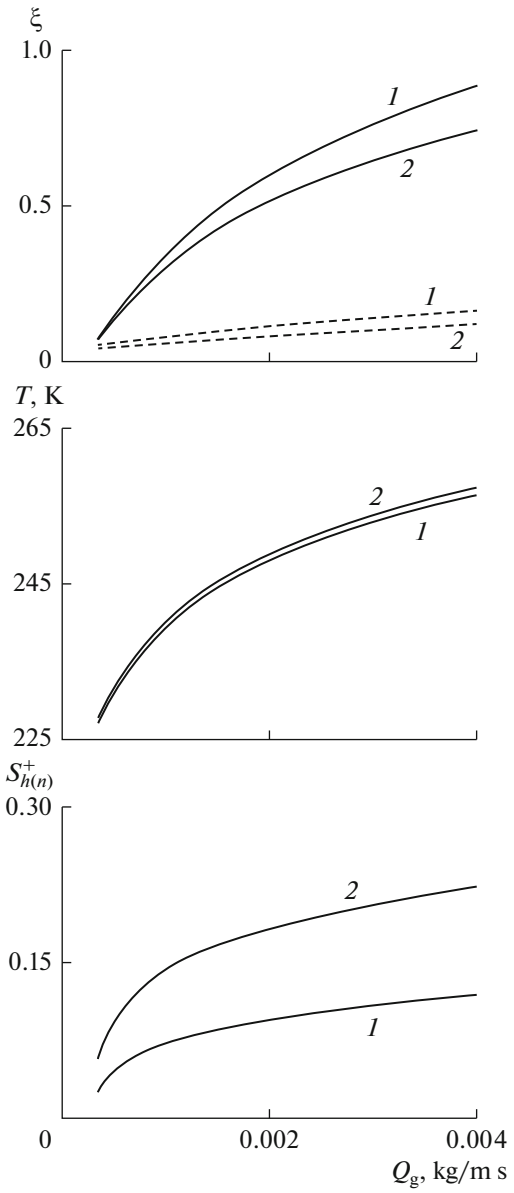

Fig. 5. Self-similar coordinates of boundaries ($\xi_{(n)}$ is near boundary (dashed line) and $\xi_{(d)}$ is distant boundary (solid line)), maximum temperatures realized in massif, and hydrate saturation at near boundary over gas mass flow rate Q_g for different initial values of snow saturation in massif S_{i0}: *1* is for 0.3 and *2* is for 0.5.

zone of hydrate formation increases, and some growth in the value of hydrate saturation $S^+_{(n)}$ is observed at the near boundary.

The dependences of the self-similar coordinates of the boundaries, the maximum temperature realized in the massif, and hydrate saturation at the near boundary on the gas mass flow rate Q_g are presented in Fig. 5 for different initial values of the snow saturation of the massif S_{i0}. It is established that, as the gas mass flow rate increases, the elongations of the spatial zone of hydrate formation and of the near zone increase and become larger the lower the initial snow saturation.

8. CONCLUSIONS

It was shown that, when a hydrate-forming gas is injected in the snow massif saturated by the same gas, the generation of three characteristic zones in the filtration region is possible: the near zone, saturated by the gas and hydrate; the intermediate zone, where the snow and hydrate are in the state of phase equilib-

rium; and the distant zone, filled with gas and snow. The self-similar solutions for the axisymmetric formulation that describe the distributions of the main parameters in the massif were constructed. It was demonstrated that an increase in the mass flow rate of the injected gas and a decrease in the initial temperature of the massif lead to the growth in both the elongation of the spatial zone of hydrate formation and the hydrate saturation at the near boundary. It was also established that, as the snow fracture in the massif grows, an increase in the elongation of the phase transition zone is observed.

REFERENCES

1. V. A. Istomin and V. S. Yakushev, *Gas Hydrates in Natural Conditions* (Nedra, Moscow, 1992) [in Russian].
2. A. V. Egorov, A. N. Rozhkov, P. R. Vogt, and K. Krejn, "Gas hydrates directly on the seabed. Natural phenomenon and theoretical justification," Preprint (Inst. Mech. Probl. RAS, Moscow, 2012).
3. O. M. Khlystov, A. V. Khabuev, O. V. Belousov, M. A. Grachev, S. Nishio, H. Sugiyama, and A. Y. Manakov, "The experience of mapping of baikal subsurface gas hydrates and gas recovery," Russ. Geol. Geophys. **55**, 1122–1129 (2014).
4. YU. F. Makogon and R. Yu. Omel'chenko, "Messoyakha - gas hydrate deposit, role and significance," Geol. Polezn. Iskopaem. Mirov. Okeana, No. **3**, 5–19 (2012).
5. M. G. Ivanov, G. M. Chudakov, I. A. Tereshchenko, A. V. Polyakov, M. S. Stepanov, and N. D. Hanyuchenko, "Problems of industrial development of natural metanogidrat," Nauch. Tr. KubGTU, No. **2**, 296–309 (2017).
6. K. Yamamoto, T. Kanno, X. X. Wang, M. Tamaki, T. Fujii, S. S. Chee, X. W. Wang, V. Pimenov, and V. Shako, "Thermal responses of a gas hydrate-bearing sediment to a depressurization operation," R. Soc. Chem. **7**, 5554–5577 (2017).
7. E. A. Bondarev, I. I. Rozhin, V. V. Popov, and K. K. Argunova, "Assessment of possibility of natural gas hydrates underground storage in permafrost regions," Kriosfera Zemli **19** (4), 64–74 (2015).
8. S. Nakai, "Development of natural gas hydrate (NGH) supply chain," in *Proceedings of the 25th World Gas Conference, Kuala Lumpur, Malaysia, June 4–8, 2012,* pp. 3040–3050.
9. M. E. Semenov, E. YU. Shic, and A. F. Safronov, "Investigation of synthesis features of methane and ethane hydrates under free convection conditions," Gazokhimiya, No. **1**, 18–23 (2011).
10. V. Sh. Shagapov, O. A. Shepelkevich, and A. V. Yalaev, "The initial stage of hydrate formation in liquid volume on impurity particles upon contact of gas and water," Theor. Found. Chem. Eng. **51**, 448–457 (2017).
11. F. F. Nazmutdinov and I. L. Habibullin, "Mathematical modeling of gas desorption from gas hydrate," Izv. Akad. Nauk, Mekh. Zhidk. Gaza, No. 5, 118–125 (1996).
12. V. Sh. Shagapov, A. S. Chiglintseva, and V. R. Syrtlanov, "Possibility of gas washout from a gas-hydrate massif by circulation of warm water," J. Appl. Mech. Tech. Phys. **50**, 628–637 (2009).
13. V. Sh. Shagapov, N. G. Musakaev, and M. K. Khasanov, "Forcing gas into a porous tank saturated with gas and water," Teplofiz. Aehromekh. **12**, 645–656 (2005).
14. V. Sh. Shagapov, G. R. Rafikova, and M. K. Khasanov, "On the theory of formation of gas hydrate in partially water-saturated porous medium when injecting methane," High Temp. **54**, 858–866 (2016).
15. V. Sh. Shagapov, A. S. Chiglintseva, and S. V. Belova, "The problem of gas hydrate formation in a closed volume saturated with gas and snow," Vestn. Tomsk. Univ., Mat. Mekh. **46**, 86–101 (2017).
16. V. Sh. Shagapov, A. S. Chiglintseva, and S. V. Belova, "Mathematical modelling of injection gas hydrate formation into the massif of snow saturated the same gas," Tr. Inst. Mekh. Mavlyutova UNTs RAN **11**, 233–239 (2016).
17. M. K. Khasanov, "Investigation of regimes of gas hydrate formation in a porous medium, partially saturated with ice," Thermophys. Aeromech. **22**, 245–255 (2015).
18. M. K. Khasanov and M. V. Stolpovskij, "Numerical simulation of hydrate formation in a finite extent porous medium partially saturated with ice," Nauch. -Tekh. Vestn. Povolzh'ya, No. **6**, 34–37 (2015).
19. V. Sh. Shagapov and O. R. Nurislamov, "Some features of the synthesis of gas hydrates by gas injection into a moist porous medium," Theor. Found. Chem. Eng. **44**, 260–271 (2010).
20. V. Sh. Shagapov and A. S. Chiglintseva, "On injection of hydrate-forming gas into a gas-saturated snowy agglomerate while transition through the ice melting point," Thermophys. Aeromech. **25**, 89–104 (2018).
21. A. S. Chiglintseva, "Self-similar solution of the problem of hydrate formation in snow massifs," Vychisl. Mekh. Sploshn. Sred **10**, 212–224 (2017).
22. A. S. Chiglintseva and V. Sh. Shagapov, "About of the injection of hydrate-forming gas into a layer of snow saturated with the same gas," Tr. Inst. Mekh. Mavlyutova UNTs RAN **12**, 219–226 (2017).
23. V. Sh. Shagapov, A. S. Chiglintseva, and A. A. Rusinov, "Mathematical modeling of hydrate formation in a reservoir saturated with snow by cold gas injection," Vychisl. Mekh. Splosh. Sred **9**, 173–181 (2016).
24. I. K. Gimaltdinov and M. K. Khasanov, "Mathematical model of the formation of a gas hydrate on the injection of gas into a stratum partially saturated with ice," J. Appl. Math. Mech. **80**, 57–64 (2016).

25. V. Sh. Shagapov, M. K. Khasanov, and N. G. Musakaev, "Formation of a gas hydrate due to injection of a cold gas into a porous reservoir partly saturated by water," J. Appl. Mech. Tech. Phys. **49**, 462–472 (2008).
26. V. Sh. Shagapov and N. G. Musakaev, *Dynamics of Formation and Decomposition of Hydrates in Gas Production, Transportation and Storage Systems* (Nauka, Moscow, 2016) [in Russian].
27. G. G. Tsypkin, *Flows with Phase Transitions in Porous Media* (Fizmatlit, Moscow, 2009) [in Russian].
28. R. I. Nigmatulin, *Dynamics of Multiphase Media* (Nauka, Moscow, 1987; CRC, Boca Raton, FL. 1990), Part 2.
29. P. I. Rahimly, Yu. A. Poveshchenko, O. R. Rahimly, V. O. Podryga, G. I. Kazakevich, and I. V. Gasilova, "The use of splitting with respect to physical processes for modeling the dissociation of gas hydrates," Math. Model. Comput. Simul. **10**, 69–78 (2018).
30. V. I. Darishcheva, V. I. Kokoreva, A. M. Polishchuk, O. V. Chubanova, and S. E. Yakush, "Modeling of filtration processes during the cyclic operation of an oil production well," Math. Model. Comput. Simul. **8**, 725–733 (2016).
31. V. Sh. Shagapov, M. N. Galimzyanov, and M. N. Zapivahina, "Simulation of ice formation during injection of water in porous media saturated with ice and gas," Vestn. Bashkir. Univ. **18** (1), 22–26 (2013).

Translated by E. Oborin